

Movements of Molecular Motors

Reinhard Lipowsky

MPI für Kolloid- and Grenzflächenforschung
14424 Potsdam, Germany *

Source:

In *Biological Physics 2000*

ed. by V. Sayakanit, L. Matsson, and H. Frauenfelder;
(World Scientific Publ. Comp., Singapore, 2001)

Abstract. The movements of cytoskeletal motors such as kinesin or myosin V cover many length and time scales. When such a motor is bound to a filament, the consumption of a single fuel molecule leads to a certain motor displacement or step which is of the order of several nanometers. The motor typically makes about a hundred such steps in its bound state and, in this way, covers a walking distance which is of the order of micrometers. On even larger length scales, the motor undergoes random walks which consist of alternating sequences of bound and unbound motor states, i.e., of directed walks along the filaments and nondirected diffusion in the aqueous solution.

1 Introduction

The living cell is a rather complex structure built up from macromolecules and supramolecular aggregates (or colloids) in aqueous solution. From the physical point of view, the most amazing property of this structure is its high degree of spatial organization or 'order' which is maintained in a stationary state far from equilibrium.

It has been realized during the last decade that this order is sustained, to a large extent, by molecular motors which consume 'fuel' molecules such as ATP and perform mechanical work within the cell. It is now believed that all transport processes or movements which occur within the cell in a coherent fashion are governed by such motors. Examples are the transmembrane transport of ions and macromolecules, the regulated adhesion and fusion of membranes, the intracellular transport of vesicles and organelles, cell division, and cell locomotion. [1] Thus, these motors act like little mechanical robots and resemble the microscopic demons envisaged by Maxwell.

There are several classes of motors which fulfill different functions within the cell: (i) DNA and RNA polymerases which move along the strands of these biopolymers; (ii) membrane pumps which transport ions and small molecules

*Email: lipowsky@mpikg-golm.mpg.de



Figure 1: Cartoon of two kinesin molecules bound to a microtubule. The microtubule is a hollow tube with a thickness of about 25 nm; it consists of tubulin dimers which have a linear size of about 8 nm. Each kinesin molecule has two heads or motor domains which can bind to the microtubule; the two heads are connected via a neck region to a long stalk which is about 50 nm.

across membranes; the resulting concentration gradients may be used in order to drive (iii) rotary motors such as the bacterial flagellar motor and the F_1 -ATPase which are used for cell locomotion and ATP synthesis, respectively; (iv) myosins in muscles which work in groups and collectively displace actin filaments; and (v) cytoskeletal motors which bind to cytoskeletal filaments and then walk along these filaments in a directed fashion. The latter class of motors is responsible for the directed transport of vesicles and other types of cargo across the cell. This nonequilibrium transport on the micrometer scale is powered by the free energy released from ATP hydrolysis on the subnanometer scale.

In the following, I will focus on cytoskeletal motors which are processive in the sense that they make many steps before they detach from the filaments. It has been estimated that a typical eucaryotic cell might contain between fifty and a hundred different types of proteins which act as such motors [2]. One example is provided by dimeric kinesin which moves along microtubules. A cartoon of the kinesin-microtubule system is shown in Fig. 1.

Two types of cytoskeletal motors, namely dimeric kinesin on microtubules [3] and myosin V on actin filaments, [4] were observed to walk via discrete steps, the size of which is close to the repeat distance of the filament which is 8 nm and 36 nm, respectively. The average velocity of these walks depends on the ATP concentration and on the applied load force; its maximal value is of the order of 1 μm per second and is obtained for high ATP concentrations and zero load force.

At each step, the cytoskeletal motor has a small but nonzero probability to unbind from the filament. Thus, its directed movement can be characterized

by a walking time Δt_b , which is the average time period between binding and unbinding, and a corresponding walking distance Δx_b along the filament. For all cytoskeletal motors studied so far, Δt_b was found to be of the order of seconds and Δx_b to be of the order of micrometers [5, 6, 7, 4, 8]. On larger time scales, the motor undergoes random walks which consist of alternating sequences of bound and unbound motor states, i.e., of directed walks along the filaments and nondirected diffusion in the aqueous solution.

This article is organized as follows. First, it is emphasized in Section 2 that the movements of molecular motors involve a wide range of different length (and time) scales. The directed walks of bound motors are discussed in Section 3. It is argued that these walks exhibit some motor properties which are universal in the sense that they are insensitive to many features of the molecular dynamics. [9, 10, 11] The random walks arising from the sequence of bound and unbound motor states are considered in Section 4.

2 Different types of movements

The movements of molecular motors cover many length and time scales. For cytoskeletal motors as considered here, one can distinguish three different regimes: (i) the molecular dynamics related to the chemomechanical energy transduction; (ii) the directed walks along the filaments; and (iii) the random walks arising from the unbinding and rebinding of the motors to the filaments.

The molecular dynamics regime (i) covers all length scales up to the motor displacement arising from the ATP hydrolysis. Experiments on dimeric kinesin strongly indicate that the hydrolysis of one ATP molecule leads to a center-of-mass displacement or step size $\ell_b = 8$ nm which corresponds to the repeat distance of the microtubule (here and below, the subscript b means 'bound'). The corresponding step time τ_b depends on the ATP concentration and on the external load force. For high ATP concentration and low load force, one finds the step time $\tau_b \simeq 6$ ms.

The directed walk regime (ii) contains the intermediate length scales which lie between the step size ℓ_b and the walking distance Δx_b . As mentioned, the walking distance is of the order of micrometers for all cytoskeletal motors studied so far; the corresponding walking times Δt_b are of the order of seconds. For dimeric kinesin derivatives without tails, the experimentally determined values are $\Delta x_b \simeq 2 \mu\text{m}$ and $\Delta t_b \simeq 2.6$ s [6].

Finally, those length and time scales, which exceed the walking distance Δx_b and the walking time Δt_b , define the random walk regime (iii). This latter regime applies to the intracellular transport of vesicles and organelles which typically involves transport over tens of micrometers. An extreme case is provided by neurons and the transport along their axons as schematically shown in Fig. 2. Axons are tube-like structures enclosed by the plasma membrane of the neuron. The axon diameter varies between hundreds of nanometers and millimeters. Their length

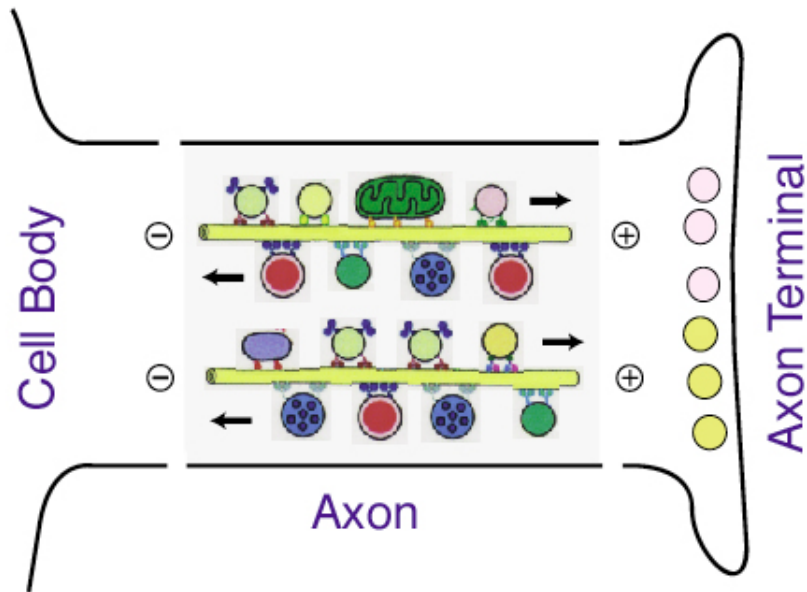


Figure 2: Schematic view through an axon which contains many microtubules, all oriented with their plus ends towards the axon terminal and with their minus ends towards the cell body. Cytoskeletal motors (indicated by small 'feet') are responsible for the transport of vesicles and organelles along these filaments.

is usually much larger than their diameter and can be up to many decimeters.

3 Directed Walks of Bound Motors

In their bound states, the cytoskeletal motors undergo directed walks along the filaments. For dimeric kinesin, this directed movement has been observed in various types of assays [12, 3, 13, 14, 15, 16, 17, 18]. This experimental work has provided several clues (i) to the biochemical and geometric features, which characterizes this motor on molecular scales, and (ii) to the transport properties which characterize the motor performance on supramolecular scales.

3.1 Experiments on dimeric kinesin

First, let us look at the kinesin–microtubule system on the molecular scale as schematically shown in Fig. 1. Each dimeric kinesin consists of two identical amino–acid chains. The amino–terminal ends of these chains correspond to the motor domains or heads which have a size of about $7 \times 4.5 \times 4.5 \text{ nm}^3$ [19]. The two heads are connected via a neck region to a long stalk. The neck region consists of ordered coiled–coil domains and a disordered hinge domain, the stalk is a coiled coil with an extension of about 50 nm.

The kinesin molecule can bind to a microtubule. The latter tube–like filament has a thickness of about 25 nm and is built up from tubulin dimers. These tubulin

molecules form 13 parallel protofilaments which provide the different 'lanes' on the surface of the microtubule. Each protofilament or 'lane' represents a 1-dimensional lattice of binding sites with a lattice constant of 8 nm.

The kinesin molecule has two binding domains located in its two heads which can adhere to one of the binding sites of the microtubule. In addition, each head can act as an ATPase which adsorbs and hydrolyses ATP. Thus, each head has an ATP-adsorption domain and a microtubule-binding domain.

The free energy released from the ATP hydrolysis is of the order of $20 T$ (here and below, temperature is measured in energy units, i.e., the Boltzmann constant k_B is adsorbed into T .) This free energy is then transduced into a conformational transition of the motor molecule which leads to its directed movement. Dimeric kinesin requires both heads in order to make many successive steps, see, e.g., [15]. Each step corresponds to a center-of-mass movement of 8 nm [3, 13, 14]. In its rigor state, the two heads are bound to two successive lattice sites separated by 8 nm [16].

All of these experimental observations are consistent with the view that dimeric kinesin moves in a 'head-over-head' (or 'hand-over-hand') fashion, i.e., by alternating steps in which one head moves forward while the other one remains bound to the tubule. If the motor does indeed advance by this type of stepping motion, the unbound head and the center-of-mass of the motor would move by 16 nm and by 8 nm, respectively, during each step.

The relative displacement of the kinesin motor against the filament was determined by optical trap experiments. The most direct evidence comes from experiments in which the filament is firmly attached to a solid substrate and the motor molecule is anchored to a bead. This bead is grapped by optical tweezers and then brought into contact with the filament. In these experiments, one can directly measure the time evolution of the displacement of a single motor molecule (plus the attached bead). From a large number of such displacement-versus-time curves, one obtains average motor properties such as the motor velocity which characterize the motor performance on length scales which are large compared to the step size.

For dimeric kinesin, the motor velocity has been measured as a function of two control parameters. The first such parameter is provided by the ATP concentration Γ , i.e., by the concentration of the fuel molecules. The second control parameter is given by the external load force F usually applied by the optical trap.

Several experiments have shown that the motor velocity v increases monotonically with Γ and exhibits a saturation behavior. In addition, the data for zero or small F could be fitted by the hyperbolic form $v(\Gamma) \simeq v_{\max} \Gamma / (\Gamma_* + \Gamma)$. [12, 20, 14] More recently, it was found that such a fit is even possible over the whole range of accessible forces as given by $0 \leq |F| \leq 5.6$ pN provided one uses F -dependent fit parameters v_{\max} and Γ_* which leads to [18]

$$v(\Gamma, F) \simeq v_{\max}(F) \Gamma / [\Gamma_*(F) + \Gamma] \quad . \quad (3.1)$$

As far as the functional dependence on the load force F is concerned, the motor velocity is observed to decrease monotonically with increasing F as one would expect naively. However, the precise functional dependence of velocity versus force has been a matter of some controversy. One problem is related to the vectorial character of the applied force which may, in general, not act parallel to the filament. In fact, if the load force is applied to the motor via an attached bead, one always generates two force components, one which is tangential to and one which is normal to the filament [20]. The normal component of the force acts to increase the probability that the motor unbinds from the filament and may also affect the ATP hydrolysis rate. Furthermore, since the tether between the bead and the kinesin molecule is not expected to behave as a linear spring, the force applied by the optical trap may not be simply proportional to the tangential force acting on the motor molecule. Here and below, the force F is taken to be the tangential component of the force which is conjugate to the motor displacement parallel to the filament. I also use the sign convention that $F < 0$ for a load force which acts against directed walk of the motor.

The relation as given by (3.1) has two nontrivial features. First, it represents a specific functional dependence of the velocity on the *two* parameters Γ and F . Secondly, the dependence on the fuel concentration Γ is found to be rather simple. These two features raise two general questions: (i) How can one *understand* the simple $v(\Gamma)$ relationship in view of the complex molecular dynamics?; and (ii) The relation as given by (3.1) describes the data for dimeric kinesin, i.e., for one particular cytoskeletal motor. *Should such a relation hold for other motors as well?* In other words: Is this relation *specific* to kinesin or is it more *universally* valid? In order to address these questions, we have studied a rather large class of ratchet models [9, 10, 11] as discussed in the next subsection.

3.2 Stochastic (M, K) -ratchets

Within the ratchet models considered here, the directed movement of the motor is described by one spatial coordinate x . For linear motors, this coordinate describes the displacement of the center-of-mass of the motor parallel to the filament (a similar approach should apply to rotary motors where x would represent an appropriate angular coordinate). For a given value of x , the motor molecule must be bound to the filament but can still attain different conformations or internal states. These different states will be labeled by the discrete index m which can have M different values. In addition, the motor can undergo transitions between these states at the discrete set of K spatial positions per motor cycle. These (M, K) -models [9, 11, 10] represent generalizations of those studied in [21, 22, 23], which were restricted to $(M, K) = (2, 2)$.

Depending on the molecular architecture of the motor, one may identify several discrete subgroups of internal states. If the motor has only one enzymatic domain or head, this head can attain a discrete number of states corresponding to (i) no substrate, (ii) adsorbed ATP, (iii) adsorbed ADP/P, and (iv) adsorbed

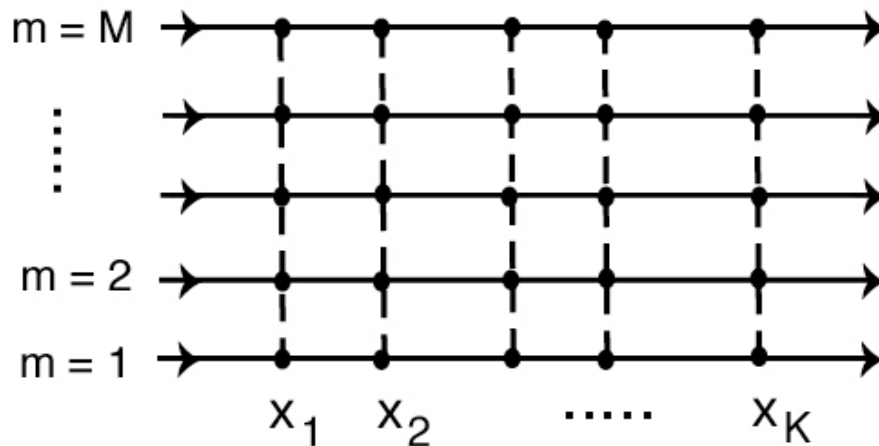


Figure 3: Network of transitions at locations $x = x_k$ with $1 \leq k \leq K$ between different internal states or levels m with $1 \leq m \leq M$. Pairs of vertices $[x_i, m]$ and $[x_j, n]$ are connected by local lateral currents for $n = m$ and $i \neq j$ (corresponding to the full lines), and by local transition currents for $i = j$ and $n \neq m$ (corresponding to the broken lines). These currents obey a vertex rule which corresponds to Kirchhoff's first law for electric circuits. The arrows represent the periodic boundary conditions in the lateral direction.

ADP. In each of these states, the motor may adopt a different conformation which will experience different interactions with the filament. If the motor has two heads, a and b , one has three groups of levels corresponding to (I) two bound heads, (II) bound head a , and (III) bound head b .

In general, the motor conformation also involves internal degrees of freedom which vary in a continuous fashion. For example, one may tilt a two-headed motor molecule, which is bound by one head, and simultaneously move its unbound head without changing the position of its center-of-mass. In the theoretical framework considered here, these continuous degrees of freedom are also discretized. This is primarily done for computational convenience. However, this discretization can involve a large number M of internal states and a large number K of transition locations corresponding to many intermediate states, and, thus, does not represent a real limitation compared to a continuous description. [†]

Within the (M, K) -ratchets, the time evolution of the motor position x and its internal state m is described by the probability densities $P_m(x, t)$ to find the motor particle at center-of-mass coordinate x and in internal state (or level) m . This probability density may change (i) because of thermally-excited diffusion within the internal state m or (ii) because of transitions between the different internal states. The probability currents arising from these different processes form a 2-dimensional network of transitions as shown in Fig. 3.

[†]A general theoretical framework in terms of continuous variables or coordinates was recently discussed in [24].

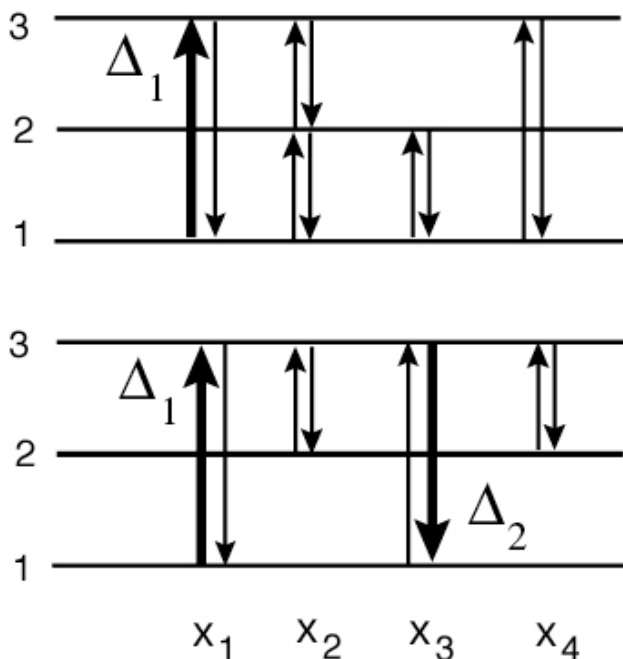


Figure 4: Transition networks with $M = 3$ internal states and (top) $Q = 1$ or (bottom) $Q = 2$ unbalanced transitions. In both examples, the balanced and unbalanced transitions are indicated by thin and thick arrows, respectively. The unbalanced rate constants are denoted by Δ_q with $1 \leq q \leq Q$.

3.3 Universal or generic aspects

A detailed investigation of the (M, K) ratchets shows that they exhibit some generic or universal transport properties which hold for *arbitrary* values of M and K . [10] In particular, it is possible to determine the explicit dependence of the motor velocity on the transition rates of the unbalanced transitions, i.e., of those transitions which arise from the enzymatic activity and which do not satisfy detailed balance.

In general, there will be Q such transition rates per motor cycle. These unbalanced transition rates will be denoted by Δ_q with $q = 1, 2, \dots, Q$, see Fig. 4. The simplest situation is provided by motors, such as monomeric kinesin, which have a single enzymatic domain. Such motors should have only one location x_k with only one unbalanced transition rate which implies $Q = 1$, see Fig. 4. There are several cytoskeletal motors such as dimeric kinesin, dynein, or myosin V which have two identical enzymatic domains or heads. The corresponding ratchet models are characterized by two (usually different) locations with enzymatic activity. If each head can make (i) only forward steps or (ii) both forward and backward steps, it can be activated (i) at only one of these locations or (ii) at both locations, which corresponds to $Q = 2$ and $Q = 4$, respectively, see Fig. 4.

Using a transfer matrix formalism, the motor velocity v is found to have the

general form [10]

$$v = \frac{\mathcal{A}(\Delta_1, \Delta_2, \dots, \Delta_Q)}{\mathcal{B}(\Delta_1, \Delta_2, \dots, \Delta_Q)} \quad (3.2)$$

where both \mathcal{A} and \mathcal{B} are two polynomials which are *multilinear* in the Q arguments Δ_q . Thus, the highest order terms which can (but need not) appear in these polynomials are proportional to the product $\prod_{q=1}^Q \Delta_q$. The functional relationships as given by (3.2) are *universal* in the sense that they hold for ratchets with arbitrary values of M and K and, thus, for any number of balanced transition rates provided one has the same number Q of unbalanced transition rates. Likewise, these relationships do not depend on the specific shapes of the molecular interaction potentials which the filament exerts onto the motor in its various internal states.

It is also important to note that the velocity–rate relationships as given by (3.2) do not involve *any* assumptions about the enzyme kinetics underlying the unbalanced transition rates. However, in order to relate the behavior of the (M, K) –ratchets to experiments, one must implement the underlying chemical kinetics which implies a certain dependence of the unbalanced rate constants Δ_q on the concentration Γ of the fuel molecules and on the applied load force F . The simplest scheme for an enzymatic reaction between the fuel molecules and the motor domain(s) is provided by Michaelis–Menten kinetics [25] which implies that $\Delta_q^{-1} = (c_q \Gamma)^{-1} + d_q^{-1}$ with $1 \leq q \leq Q$ where the reaction rates $c_q = c_q(F)$ and $d_q = d_q(F)$ will, in general, depend on the load force F .

If one uses these Michaelis–Menten relations, one obtains the general velocity–concentration relationship as given by [10]

$$v(\Gamma, F) = \left[\sum_{n=0}^Q g_n(F) \Gamma^n \right] / \left[\sum_{n=0}^Q h_n(F) \Gamma^n \right] \quad (3.3)$$

which represents the ratio of two Γ –polynomials of degree Q with F –dependent coefficients. The first polynomial coefficient g_0 in the numerator satisfies $g_0(F = 0) = 0$. If the motor cycle exhibits certain symmetries or constraints, some polynomial coefficients may vanish for all values of F .

The relationships as given by (3.3) are again *universal* in the sense that they are valid (i) for any number of balanced transition rates, (ii) for any choice of the molecular interaction potentials, (iii) for arbitrary load force F , and (iv) for any force dependence of the Michaelis–Menten reaction rates c_q and d_q .

As mentioned, the simplest motor cycles are characterized by $Q = 1$. In this case, the relation (3.3) simplifies and reduces to

$$v(\Gamma, F) = [g_0(F) + g_1(F)\Gamma] / [h_0(F) + h_1(F)\Gamma] \quad . \quad (3.4)$$

For $F = 0$, one has $g_0(F = 0) = 0$ which implies

$$v(\Gamma, 0) = v_{\max} \Gamma / [\Gamma_* + \Gamma] \quad . \quad (3.5)$$

with the saturation velocity $v_{\max} \equiv g_1(0)/h_1(0)$ and the characteristic concentration $\Gamma_* \equiv h_0(0)/h_1(0)$.

The rather simple velocity–concentration relationship (3.5) was first obtained from a simple tight–coupling picture [12, 20]. The latter picture is based on two assumptions: (i) the motor makes one step of mean step size Δx per ATP hydrolysis; and (ii) the ATP hydrolysis follows Michaelis–Menten kinetics which implies that its rate constant ω_{hyd} is given by $\omega_{\text{hyd}}(\Gamma) = \omega_{\max}\Gamma/(\Gamma_* + \Gamma)$. A combination of these two assumptions leads to

$$v(\Gamma, 0) = \Delta x \omega_{\max}\Gamma/[\Gamma_* + \Gamma] \quad (3.6)$$

which is equivalent to (3.5).

The simple tight–coupling picture just described has the disadvantage that it provides no insight into its range of validity or its limitations. In contrast, the systematic theoretical approach based on the (M, K) –ratches leads to a classification scheme which contains the simple Michaelis–Menten–type relation (3.5) as a special case. In other words, this approach characterizes both those motors for which the relationship as given by (3.5) holds exactly as well as those motors for which this relationship is replaced by more general relations as in (3.3).

The simple relationship (3.5) is always valid provided (i) the motor cycle is characterized by $Q = 1$ and (ii) this unbalanced rate follows Michaelis–Menten kinetics. If (ii) remains valid but $Q \geq 2$, one should, in general, expect to see the more general relationships as given by (3.3). There are exceptional cases, however, which arise from additional symmetries and constraints within the motor cycle. Indeed, as a result of these symmetries or constraints, some of the polynomial coefficients in (3.3) may vanish for all values of F . The latter situation has been explicitly shown to apply to some models for dimeric kinesin with $(M, K) = (2, 2)$ and $(M, K) = (3, 2)$. [9, 10]

Finally, one should note that the enzymatic reaction does not necessarily follow Michaelis–Menten kinetics. One example for a different kinetics would be provided by molecular motors with allosteric domains which bind regulatory molecules. The reaction rate Δ_q can then exhibit a sigmoidal dependence on Γ [25]. If such a sigmoidal form is inserted into the general expression (3.2) for the dependence of the motor velocity v on the unbalanced transition rates Δ_q , one will obtain a v – Γ relationships which differs from (3.3).

In summary, it is possible to classify the Γ –dependence of the motor velocity v as discussed in the present subsection. Such a classification scheme is not available for the F –dependence of v which depends on the details of the interaction potentials between the filament and the motor and, thus, reflects the specific features of the underlying molecular structure. It is, however, not difficult to calculate the F –dependence of the motor velocity if one makes some specific assumptions about the interaction potentials as shown in [9] for several types of sawtooth potentials.

4 Random Walks of Motors and Motor Traffic

Even processive motors eventually unbind from the filaments. As mentioned in the introduction, this unbinding process can be characterized by a walking time Δt_b , which is of the order of seconds, and by the corresponding walking distance Δx_b , which is of the order of micrometers. Both quantities depend on the overall ionic strength [5, 8], on the presence of certain ions such as magnesium [C. Schmidt, M. Rief, private communication], and on the molecular roughness of the filaments arising from adsorbed tau proteins [7] or from chemically altered tubulin [8].

4.1 Diffusion of unbound motors

A motor which is no longer bound to the filament, will undergo diffusive motion in the surrounding liquid. For an in vitro system, the corresponding diffusion coefficient D_{ub} is given by the classical Stokes–Einstein relation $D_{ub} = k_B T / (6\pi\eta R_{\text{hyd}})$, see, e.g., [26], and depends on the thermal energy $k_B T$, on the dynamic viscosity η of the solution, and on the effective hydrodynamic radius R_{hyd} of the motor particle (here and below, the subscript ub means ‘unbound’ state of motor and filament). If the dynamic viscosity has a value close to $\eta \simeq 0.9$ mPa s (\equiv cP) as appropriate for pure water, one has $D_{ub} = 24 \mu\text{m}^2/\text{s}$ for a motor molecule with a hydrodynamic radius of 10 nm, and $D_{ub} = 2.4 \mu\text{m}^2/\text{s}$ for a motor with an attached bead of radius 100 nm.

It is interesting to compare these estimates for the unbound diffusion coefficient D_{ub} with the values for the bound state diffusion coefficients D_b as measured for kinesin. These latter values are of the order of $10^{-3} \mu\text{m}^2/\text{s}$ [13, 6] and $5 \times 10^{-2} \mu\text{m}^2/\text{s}$ [6] for two-headed and one-headed kinesin, respectively. The relatively small values of D_b reflect the additional friction arising from the binding between motor and filament. Thus, for a normal aqueous solution, the unbound diffusion coefficient D_{ub} is much larger than the bound state diffusion coefficients D_b . In principle, one could reduce D_{ub} by a factor up to 10^{-2} if one changes the viscosity of the aqueous solution by adding some solutes such as glycerol or sucrose.

It is more difficult to estimate the diffusive motion of an unbound motor in vivo. The cytosol contains macromolecules, supramolecular structures, and organelles, and the unbound motor may experience both repulsive and attractive interactions with these ‘particles’. For repulsive interactions, the particles represent additional steric barriers for the diffusive motion of the motor which will then exhibit a reduced diffusion coefficient. This reduction may be estimated by comparison with the diffusion of inert particles in fibroblasts for which the values $D_{ub} \simeq 1.6 \mu\text{m}^2/\text{s}$ and $\simeq 3000 \text{ nm}^2/\text{s}$ have been measured for particle radii of 10 nm and 80 nm, respectively [27]. Compared to water, this corresponds to a size-dependent reduction factor of 10^{-1} and 10^{-3} , respectively.

4.2 Tracer motors in open compartments

On time scales which are large compared to the walking time Δt_b , the motor undergoes random walks which consist of alternating sequences of bound and unbound motor states, i.e., of directed walks along the filaments and nondirected diffusion in the aqueous solution. When bound to a filament, the motor walks in a certain direction until it unbinds; it then undergoes nondirected diffusive motion in the surrounding aqueous solution until it encounters the same or another filament to which it can rebind and continue its directed walk.

It is intuitively clear that the relative importance of directed and diffusive motion will depend on the number and arrangement of the filaments and on the confinement of the motion by boundaries or walls. For 2- and 3-dimensional systems without boundaries, the corresponding motor walks were studied by Ajdari [28] using scaling arguments. For these systems without confining walls, we have been able to obtain complete analytical solutions for the time evolution of the drift velocity and of the diffusion coefficient; in addition, we also determined these quantities by Monte Carlo (MC) simulations and found very good agreement with the analytical results [29].

We have also extended these studies to bounded geometries or compartments as shown in Fig. 5 which are accessible to in-vitro experiments. [30] We explicitly considered oriented filaments which are attached to the interior surfaces of three types of *open* compartments (half space, slab, open tube) as in Fig. 5. In the half space, the motor velocity v decays $\sim 1/t$ for long times t and the advancement of the motor is so slow that it will be difficult to measure. In the slab, $v \sim 1/t^{1/2}$ and the advancement should be measurable if one tracks the motor for a couple of minutes. For an open tube which resembles an axon, the velocity is reduced by a constant factor which depends on the radius of the tube.

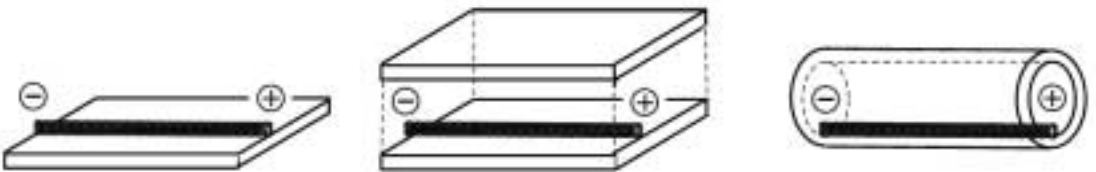


Figure 5: Various compartments with one filament attached to the confining walls: (left) half space; (middle) slab; (right) open tube. The filament corresponds to the thick rod with its minus-end on the left and its plus-end on the right. The three compartments are open in at least one spatial direction.

4.3 Motor traffic in closed compartments

Finally, let us close the orifices of the open tube in Fig. 5. One now attains a compartment which confines the motors in all three spatial directions. If an ensemble of *many* motors is placed in such a compartment, the ATP hydrolysis of the bound motors on the nanometer scale generates motor concentration gradients and motor currents on the micrometer scale. These mesoscopic gradients and currents lead to novel stationary states far from equilibrium which are characterized by a subtle balance between bound currents along the filaments and diffusive currents in the aqueous solution. [30]

For the open compartments discussed in the previous subsection, it was implicitly assumed that the motor concentration is relatively small and that one can safely ignore possible interactions between different motor particles. In contrast, if the compartment is closed, one must include the mutual exclusion of two motor particles in order to describe the motors bound to the filaments. Indeed, these filaments become easily overcrowded or 'jammed' even if the overall motor concentration is still rather small.

Acknowledgments

I thank Thomas Harms, Theo M. Nieuwenhuizen, Stefan Klumpp and Nicole Jaster for fruitful collaborations.

References

- [1] B. Alberts *et al.*, *Essential cell biology: An introduction to the molecular biology of the cell* (Garland, New York, 1998).
- [2] J. A. Spudich, *Nature* **372**, 515 (1994).
- [3] K. Svoboda, C. Schmidt, B. Schnapp, and S. Block, *Nature* **365**, 721 (1993).
- [4] A. Mehta *et al.*, *Nature* **400**, 590 (1999).
- [5] R. D. Vale *et al.*, *Nature* **380**, 451 (1996).
- [6] Y. Okada and N. Hirokawa, *Science* **283**, 1152 (1999).
- [7] B. Trinczek, A. Ebnet, E.-M. Mandelkow, and E. Mandelkow, *J. Cell Sci.* **112**, 2355 (1999).
- [8] Z. Wang and M. Sheetz, *Biophys. J.* **78**, 1955 (2000).
- [9] R. Lipowsky and T. Harms, *Eur. Biophys. J.* **29**, 542 (2000).
- [10] R. Lipowsky, *Phys. Rev. Lett.* **85**, 4401 (2000).

- [11] R. Lipowsky, in *Stochastic Processes in Physics, Chemistry and Biology*, Vol. 557 of *Lecture Notes in Physics*, edited by J. A. Freund and T. Pöschel (Springer, Heidelberg, 2000), pp. 21–31.
- [12] J. Howard, A. J. Hudspeth, and R. D. Vale, *Nature* **342**, 154 (1989).
- [13] M. J. Schnitzer and S. M. Block, *Nature* **388**, 386 (1997).
- [14] W. Hua, E. C. Young, M. L. Fleming, and J. Gelles, *Nature* **388**, 390 (1997).
- [15] W. O. Hancock and J. Howard, *J. Cell Biol.* **140**, 1395 (1998).
- [16] M. Thormählen *et al.*, *J. Mol. Biol.* **275**, 795 (1998).
- [17] S. Gilbert, M. Moyer, and K. Johnson, *Biochemistry* **37**, 792 (1998).
- [18] K. Visscher, M. J. Schnitzer, and S. M. Block, *Nature* **400**, 184 (1999).
- [19] F. J. Kull *et al.*, *Nature* **380**, 550 (1996).
- [20] K. Svoboda and S. Block, *Cell* **77**, 773 (1994).
- [21] J. Prost, J.-F. Chauwin, L. Peliti, and A. Ajdari, *Phys. Rev. Lett.* **72**, 2652 (1994).
- [22] F. Jülicher, A. Ajdari, and J. Prost, *Rev. Mod. Phys.* **69**, 1269 (1997).
- [23] A. Parmeggiani, F. Jülicher, A. Ajdari, and J. Prost, *Phys. Rev. E* **60**, 2127 (1999).
- [24] D. Keller and C. Bustamante, *Biophys. J* **78**, 541 (2000).
- [25] A. Lehninger, D. Nelson, and M. Cox, *Principles of biochemistry*, 2nd ed. (Worth Publishers, New York, 1993).
- [26] H. C. Berg, *Random walks in biology* (Princeton University Press, Chichester, 1993).
- [27] K. Luby-Phelps, *Int. Rev. Cytology - A Survey of Cell Biol.* **192**, 189 (2000).
- [28] A. Ajdari, *Europhys. Lett.* **31**, 69 (1995).
- [29] T. Nieuwenhuizen, S. Klumpp, and R. Lipowsky, submitted.
- [30] R. Lipowsky, S. Klumpp, and T. Nieuwenhuizen, *Phys. Rev. Lett.* **87**, 108101/1 (2001).